Iranian Journal of Hydrogen & Fuel Cell 3(2017) 219-230

Iranian Journal of Hydrogen & Fuel Cell

IJHFC

Journal homepage://ijhfc.irost.ir

Dynamic investigation of a hydrocarbon proton exchange membrane fuel cell

Milad Shakouri Kalfati[1], Aida Karimi[1], Soosan Rowshanzamir[2,*]

[1,2] **School of Chemical Engineering, Iran University of Science and Technology, Narmak, Tehran, Iran**
[2] **Fuel Cell Laboratory, Green Research Centre, Iran University of Science and Technology, Tehran, Iran**

Article Information

Article History:

Received:
03 Sep 2017
Received in revised form:
13 Nov 2017
Accepted:
09 Dec 2017

Keywords

Hydrocarbon proton exchange membrane
Fuel cell
SPEEK
Modeling
Dynamic

Abstract

Sulfonated polyether ether ketone (SPEEK) is categorized in a nonfluorinated aromatic hydrocarbon proton exchange membrane (PEM) group and considered as a suitable substitute for common per-fluorinated membranes, such as Nafion, due to wider operating temperature, less feed gas crossover, and lower cost. Since modeling results in a better understanding of a phenomenon, in this study a dynamic one-dimensional model of the membrane electrode assembly (MEA) of this membrane is developed. The model includes both gas and electrolyte phases. Species transfer by diffusion and convection in an intra-phase and interphases space and participate in electrochemical reactions. The catalyst layers are modeled in detail with catalyst agglomerates covered with a layer of electrolyte and feed gas transfers into the electrolyte phase by Henry's low. Then the gas diffuses to the catalyst surface on which it reacts electrochemically. The polarization curve of this MEA obtained from the model is validated against experimental data and shows acceptable agreement. Concentration profiles in the MEA both in the gas and electrolyte phase with time are also presented as results.

1. Introduction

Fuel cells have been getting more and more noticed as a green energy source in the last decade. Although proton exchange membrane fuel cells (PEMFCs) are one of the most applicable fuel cells for automotive and domestic use, they are still not competitive compared to other energy sources due to high cost.

*Corresponding Author's Fax: 0098 2177491242
E-mail address: rowshanzamir@iust.ac.ir

doi: 10.22104/ijhfc.2017.2439.1154

[1]Proton Exchange Membrane

A significant portion of PEMFC production cost is dedicated to its membrane. Commonly used per-fluorinated membranes are expensive and a vast amount of research has been conducted to find an appropriate substitute for them [1]. Sulfonated Poly Aromatic (SPA) is known as a possible alternative due to their ability to work at higher temperatures, reasonable price, and less feed-crossover. Hence, many types of research have been published recently that investigate the usage of SPAs. These polymers are also referred to as the non-fluorinated hydrocarbon PEMs, such as sulfonated polyether sulfone (SPES) [2-4], sulfonated polyether sulfone ketone [5, 6], sulfonated poly-phenyl sulfone (SPPSU) [7, 8], sulfonated polyimide (SPI) [9, 10], sulfonated polybenzimidazole (SPBI) [11, 12], and Sulfonated polyether ether ketone (SPEEK) which is one of the most distinguished SPAs, have good mechanical and thermal stability and proton conductivity.

In the previous decade SPEEK has been proven to be a promising substitute for fluorinated membranes like Nafion in PEMFCs. Many researchers have investigated in detail the process and the kinetics of the post sulfonating process of PEEK. Huang et al. studied the post-sulfonation process of PEEK at different temperatures [13]. They reported that the sulfonation reaction is a second order reaction and obtained the reaction rate coefficient. Gil et al. investigated the direct synthesis of SPEEK by polymerization of the sulfonated monomer [14]. Xing et al. compared the properties of SPEEK obtained by post-sulfonation of two different commercial PEEKs in various degree of sulfonation [15]. Lakshmi et al. also investigates the thermal decomposition of a SPEEK membrane obtained by post-sulfonation of PEEK with DS 70-80% [16]. Other scientists examined the effect of the degree of sulfonation on the properties of SPEEK as a PEM. Parnian et al. represented a comprehensive study of SPEEK properties with different DS [17]. They included mechanical, electrochemical and chemical stability analysis of this membrane in various degrees of sulfonation.

SPEEK membrane is usually obtained by solution casting of a SPEEK polymer. Different solvents are utilized for this purpose such as DMAc, DMSO, DMF, NMP, and water or a mixture of water and ethanol. In a recently published paper, He et al. used a water-ethanol mix as a casting solvent for a SPEEK membrane with a high degree of sulfonation [18]. Carbone et al. compared the effect of DMAc and DMSO on the crystallinity of the resulting membrane [19]. They reported that the membrane cast by DMAc as a solvent has a low crystallinity with an amorphous structure which is preferred in PEMs [19]. Do et al. characterized SPEEK membrane cast with different solvent sand different degrees of sulfonation mechanically [20]. They reported the membrane's young module. Li et al. investigated the effect of different casting solvent on the microstructure of a SPEEK membrane [21]. Jun et al. studied how the treatment would reduce the impact of casting solvents on the SPEEK membrane properties [22].

Many researchers inspected the advantages of using SPEEK as a PEM in DMFCs due to its low methanol permeability. Li et al. reported SPEEK permeability for different species that were involved in a DMFC process, like oxygen and methanol [23]. Lee and Manthiram investigated the utilization of SPEEK both as a membrane and catalyst layer ionomer for DMFC [24]. Yang and Manthiram had previously shown that SPEEK membrane used as a PEM in DMFC could perform comparably to Nafion in certain conditions [25]. Additionally, there have been many papers focusing on the enhancement of SPEEK properties by blending it with other polymers or make a nanocomposite based on this polymer. Sayadi et al. investigated the proton conductivity and reactant gas crossover of a SPEEK self-humidifying nanocomposite [26]. Crosslinking is another alternative to enhance the mechanical behavior of SPEEK membrane. In this regard, Anderson et al. used the ion-induced method to cross-link this polymer [27].

In the field of modeling, there is previous research that has modeled SPEEK at the molecular level. Zhao et al. studied the fundamental properties of SPEEK such as proton dissociation and spectral features utilizing a molecular dynamic model [28]. Mahajan and Ganesan developed an atomistic model

to study the structure of SPEEK membrane [29]. They reported in their paper the structural characterizations of this membrane in different water and methanol content and temperature and showed that protons and molecules could transport through the membrane easier when the hydration of the membrane is high. Komarov et al. utilized both an atomistic and a mesoscale simulation of SPEEK membranes to showed that water content could affect the structure of the water channels in a fully of hydrated SPEEK membrane [30].

However, there is a lack of a macro scale model of this membrane as PEM in an MEA.

A detailed experimental investigation of an MEA is exceptionally complicated because of the multi-physics, multiphase and multi-layer nature of its transport process . This signifies the importance of modeling in this field [31].

Fuel cell modeling has been investigated for decades. Different types of models have been developed which can be categorized from various aspects. For instance, from the dimensional point of view 3, 2 and one-dimensional modeling has been used each serving diverse objectives. One dimensional model commonly used to investigate different layer of the MEA in detail mainly focuses on the membrane. Poornesh et al. modeled the mechanical degradation of a Nafion membrane [32]. The two-dimensional model usually focuses on the variation along a channel or a rib. Qin and Hassanzadeh developed a 2-dimensional model for liquid water flooding in a fuel cell [33]. Finally, 3-dimensional models have focused on overall flow channel designs, but due to high computational cost could not concentrate on details. Cao et al. modeled a fuel cell in 3-dimension to investigate the temperature distribution considering the thermal contact resistant for different layers of the cell [34]. There are models developed for fuel cells working with a hydrocarbon non-fluorinated membrane such as PBI [35, 36]. However, to the best of the author's knowledge there is still a lack of a fuel cell model working with a SPEEK membrane. Consequently, in this study a dynamic model of an MEA working with SPEEK membrane is developed in one dimension. The presented model is mainly essential for considering the interphase mass transfer between electrolyte and gas phase and assuming electrochemical reactions occurs in the electrolyte phase, which is more realistic than conventional models considering only gas phase. In this model, the fact that the remaining reactant can diffuse to the other side of the cell through the membrane layer is also considered. This phenomenon is called gas crossover and may reduce the available power of the cell.

2. Method and assumptions

The computational domain in this study is an MEA sandwich consisting of gas diffusion layers (GDL), Catalyst Layers (CL) and a proton exchange membrane (PEM). The following assumption are made to simplify the model: (I) Dynamic process, (II) The model is developed in one dimension, assuming isotropic and homogeneous porous layers (GDLs, CLs) and a membrane. The schematic diagram of model geometry is represented in Fig. 1.

Dimensions of each part of MEA are demonstrated in Table 1 .

Table 1. Structural and physical parameters used in the model.

Symbol	Quantity	Value
L_{GDL}	GDL thickness	170 μm
L_{MPL}	MPL thickness	30 μm
L_{CL}	Catalyst layer thickness	25 μm
L_{m}	Membrane thickness	50 μm

The operational condition used in the model is shown in Table 2. Feed gas concentration was obtained from eq.1. This equation is used for ideal gas and since the operating pressure is less than 5 bars, this assumption is allowable.

2.1. Governing equations

The transport phenomena in the fuel cell include mass, momentum, heat and charge transfer. The governing equation of each aspect is described as follows.

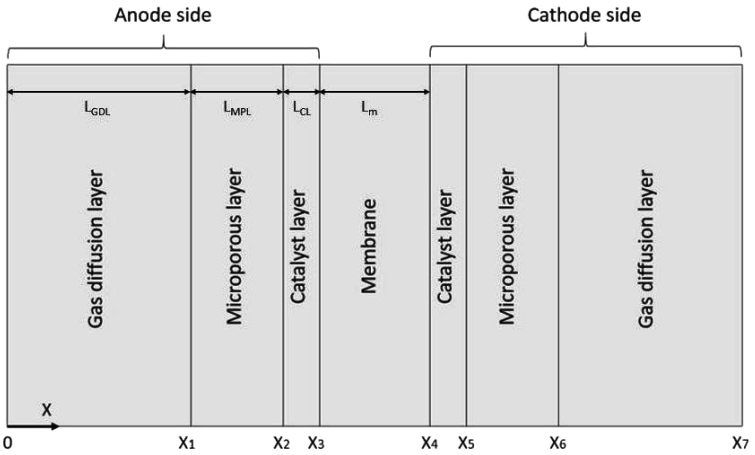

Fig.1. Schematic diagram of model geometry.

Table 2. Operating conditions used in this model.

Symbol	Quantity	Value	Ref
d	Polymer density	1 kg L^{-1}	[37]
T	Temperature	373.15 K	
P_a	Gas pressure in anode channel	2 atm	
P_c	Gas pressure in cathode channel	2 atm	
C_i	Total gas concentration in channels	$\frac{P_i}{RT}$, i = a, c (1)	
$x_{H2O,\,i}$	Mole fraction of water	$x_{H_2O,i} = \frac{P_{sat} a_{w,i}}{P_i}$, i = a, c (2)	
$C_{H2O,\,i}$	Water concentration in channels	$x_{H_2O,i} C_i$, i = a, c (3)	
C_{H2}	H_2 concentration in anode channel	$C_a - C_{H2O,\,a}$ (4)	
C_{O2}	O_2 concentration in cathode channel	$0.21(C_c - C_{H2O,\,c})$ (5)	

Mass transfer in the gas phase:

$$\frac{\partial}{\partial t}\left(\varepsilon c_{g,j}\right) - \frac{\partial}{\partial x}\left[\varepsilon^{3/2} D_j \frac{\partial c_{g,j}}{\partial x} - \nu_g c_{g,j}\right] = R_j \qquad (6)$$

Where $c_{g,j}$ denotes the concentrations of species, j=O_2, H_2, N_2 and H_2O. D_j is the free space diffusion coefficient of the component j and ε is the porosity of the layer, whose value is 0.74, 0.3 and 0.2 for GDL, MPL and catalyst layers, respectively. Source and sink terms are related to the solution of the species in the ionomer phase or vice versa (Table 3).

The Darcy equation is used to show momentum transfer in the gas phase.

$$p\vec{u} = -\left(\frac{\kappa}{\mu}\right)\nabla P \qquad (7)$$

Table 3. Source and sink terms of species in the gas phase.

	ACL/CCL	descriptions
R_{H2O}	$-h_{pc}\left(x_{vP} - P_{sat}\right)$	distillation/ vaporization
R_{H2}	$h_{pe,H}\left(H_H c_H - c_{H,e}\right)$	absorption/ desorption
R_{O2}	$h_{pe,O}\left(H_O c_O - c_{O,e}\right)$	absorption/ desorption

In this equation, κ is the absolute permeability and μ is the dynamic viscosity.

In the electrolyte phase, the mechanism of species transfer is the only diffusion. Therefore, the equation of mass transfer for this phase is:

$$\frac{\partial}{\partial t}\left(\varepsilon c_{e,j}\right) - \frac{\partial}{\partial x}\left[\varepsilon^{3/2} D_j \frac{\partial c_{e,j}}{\partial x}\right] = R_j \qquad (8)$$

$$j = H_2,\ O_2,\ H_2O,\ H_2O_2,\ OH$$

$$\frac{\partial}{\partial t}\left(c_{m,j}\right)-\frac{\partial}{\partial x}\left[D_j\frac{\partial c_{m,j}}{\partial x}-z_j u_{m,j}Fc_{m,j}\frac{\partial V}{\partial x}\right]=0$$
$$u_{m,H_2O}=\frac{5\lambda\sigma_e}{44c_{H_2O}F^2},\quad u_{m,j}=0\quad j\neq H_2O \tag{9}$$

In which z_j, u_{mj}, F, V are, respectively, ionic charge, mobility, Faraday constant and electrical potential. R_j is the source and sink of species in this phase, as shown in Table 4. At the membrane, the proton is usually attached to the water molecules and produces the hydronium ion. Then the hydronium ion transfer through the membrane both because of concentration gradian and the potential field between the anode and cathode. During this transfer, the hydronium ion would drag some water molecules, too.

Equation (10) is used to consider the charge transfer in MEA.

$$-\frac{\partial}{\partial x}\left(\varepsilon^{\frac{3}{2}}\sigma_e\frac{\partial\phi}{\partial x}\right)-S_\phi=-\frac{\partial}{\partial x}\left(\varepsilon^{\frac{3}{2}}\sigma_S\frac{\partial\psi}{\partial x}\right)-S_\psi=0 \tag{10}$$

$$i=i_0\left(\frac{c_R}{c_{ref,R}}\exp\left(\frac{\alpha_a F\eta}{RT}\right)-\frac{c_O}{c_{ref,O}}\exp\left(\frac{-\alpha_c F\eta}{RT}\right)\right) \tag{11}$$

$$\eta=\psi-\phi-E_0 \tag{12}$$

$$I=\int a_j i\,dx \tag{13}$$

In the above equations $\sigma_e,\sigma_s,\varphi,\psi,S_\varphi,S_\psi$ are the proton, electron conduction, electric and ionic potentials, respectively. In eq.13, i is the local current produced by the concentrated dependent Bulter Volmer equation [38], and α_a, α_c, C_R, C_O, η and E_0 are anodic and cathodic current exchange coefficient, reductant and oxidant concentrations, activation overpotential and thermodynamic potential, respectively. The cell produced current can be calculated from Eq. (13) in which a_j is the specific area of the catalyst.

One of the important fuel cell membrane parameters is proton conductivity. The proton conductivity of the membrane is a function of the water content and temperature. Equation 14, developed by the authors, shows the relationship of this variable gives the proton conductivity of the SPEEK membrane.

$$\sigma_{sPEEK}\left[\frac{S}{cm}\right]=\frac{96.485\,d}{Mw_{H_2O}.\,\lambda}\exp\left(a(T)\left(\frac{1000\,d}{Mw_{H_2O}.\,\lambda}\right)^{0.5}+b(T)\right) \tag{14}$$

$$a(T)=\frac{2.7054\times10^{-5}\,T^2-2.4595\,T+37.8726}{T-16.7594} \tag{15}$$

$$b(T)=-14.7043\,T^{-0.1535}+3.3413 \tag{16}$$

Where T is the operating temperature and λ is the water content of the membrane. And finally, equation 17 is used to consider the heat transfer and its effect on the MEA .

$$\frac{\partial}{\partial t}\left(\varepsilon\rho_g C_g T+\rho_s C_s T\right)+\frac{\partial}{\partial x}\left(\varepsilon\rho_g C_g T\right)-\frac{\partial}{\partial x}\left(k\frac{\partial T}{\partial x}\right)=S_{act}+S_{rev}+S_{ohm}+S_{pc} \tag{17}$$

$$k=k_p\varepsilon+k_e\varepsilon_e+k_a\varepsilon_a \tag{18}$$

Table 4. Source and sink of species in catalyst layers of ionomer phase.

ACL	CCL	description
R_{H2}	$-h_{pe,H}\left(H_H c_H-c_{H,e}\right)$	adsorption/desorption
	$-\frac{v_{H_2}.\,i}{n.\,F}-q_c$ $\quad -q_c$	consumption of hydrogen
R_{O2}	$-h_{pe,O}\left(H_O c_O-c_{O,e}\right)$	adsorption/desorption
	$-\frac{v_{O_2}.\,i_{2e}}{2\,F}-q_c$ $\quad -\frac{v_{O_2}.\,i_{4e}}{4\,F}-\frac{v_{O_2}.\,i_{2e}}{2\,F}-q_c$	consumption of oxygen

where C_g, C_s and ρ_g, ρ_s are the heat capacity and density of the gas phase and solid phase. k is the heat conduction coefficient that can be obtained by a volumetric average of k_p, the porous matrix, k_e, the electrolyte and k_a, the agglomerates heat conduction coefficients The source and sink for the energy equation are showed in Table 5.

3. Results and Discussion

Our model consists of the different transfer phenomena involve in a PEMFC process and with the above governing equations solved numerically results in concentration profiles. Fig.2 and Fig. 3 present the feed concentration profile in the gas phase through an MEA at different times. In GDL and MPL there is no net consumption or production; hence, the mass transfer is governing by diffusion and convective mass transfer. Without any sour or sink concentration profiles are expected to be linear, which is compatible with the results of the model. However, in CLs mass transfer from the gas phase to the electrolyte phase acts as the net sink. Therefore, the slope of concentration of oxygen and hydrogen in the cathode and anode side varies along the CLs.

As it is shown in Fig.2 and Fig.3 , the model assumes a constant concentration of gases as the initial condition.

In the course of time the variation of the profile decreases. Eventually the profiles reach the point that the difference is small enough to consider the processes in the fuel cell steady, and change to the point that it reaches to the SteadyState conditions.

After dissolving Hydrogen and Oxygen in the CLs, this material could participate in the electrochemical reaction. Fig.4 and Fig.5 demonstrate reactant concentration profiles in the electrolyte phase in which mass transfer from the gas phase is considered as a source and electrochemical reactions as the sink. In Fig. 4 the concentration of Hydrogen in the electrolyte phase changes with time until it reaches the steady-state conditions in the same way that the gas phase concentration did. Additionally, the slope of the concentration profile changes in the ACL due to the dissolving of the gaseous hydrogen into the electrolyte phase, it is also consumed by the electrochemical reaction. However, this effect is not significant due to high concentration change through the membrane layer. In the CCL, the transfer of Hydrogen into the gas phase from the electrolyte is considered, and as a resultits concentration in this part has a low value and is almost equal to zero.

The same procedure is valid for Oxygen concentration in the electrolyte phase with the difference being that oxygen is introduced into the cell in cathode side then it dissolves into the electrolyte in the catalyst layer and is involved in the electrochemical reaction. Then the remaining oxygen would diffuse through the membrane to the anode side. Fig.5 demonstrates Oxygen concentration profiles in the electrolyte phase in which mass transfer from the gas phase is considered as a source and electrochemical reactions as the sink. As it is shown in Fig. 5, the higher activation barrier of oxygen oxidation reaction caused more concentration difference in the cathode

Table 5. Source and sink for the energy equation.

	Membrane	Catalyst layers	GDL/MPL	Meaning
S_{act}	0	$F\eta_j R_j\left(\eta_j, T, C^s_{i,e}\right)$	0	Activation losses
S_{rev}	0	$-\Delta_j T R_j\left(\eta_j, T, C^s_{i,e}\right)/n$	0	Heat of reaction
S_{ohm}	$\sigma_e(\partial\phi/\partial x)^2$	$\epsilon_e^{1.5}\sigma_e(\partial\phi/\partial x)^2+\epsilon_c^{1.5}\sigma_s(\partial\psi/\partial x)^2$	$\left(1-\epsilon_g/\epsilon_{mp}\right)^{1.5}\sigma_s(\partial\psi/\partial x)^2$	Ohmic losses
S_{pc}	0	$h_{gl}h_{pc}\left(X_{vP}-P_{sat}\right)$	$h_{gl}h_{pc}\left(X_{vP}-P_{sat}\right)$	Heat of evaporation

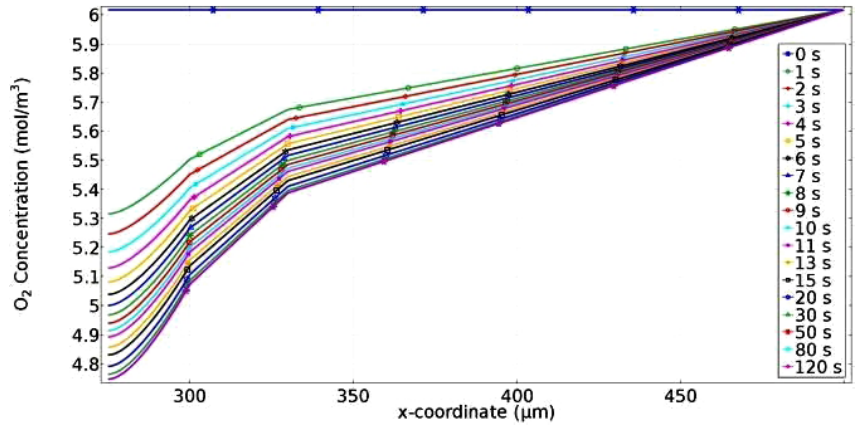

Fig. 2. Concentration profiles of O_2 in the cathode at different times.

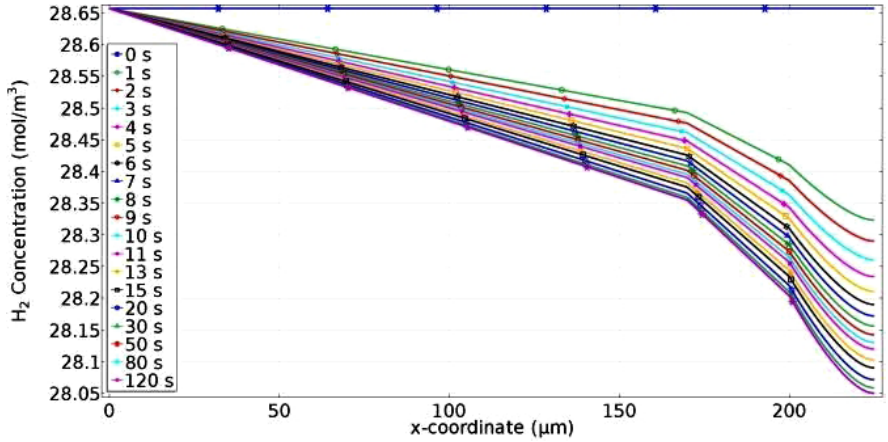

Fig. 3. Concentration profiles of H_2 in the gas phase at different times.

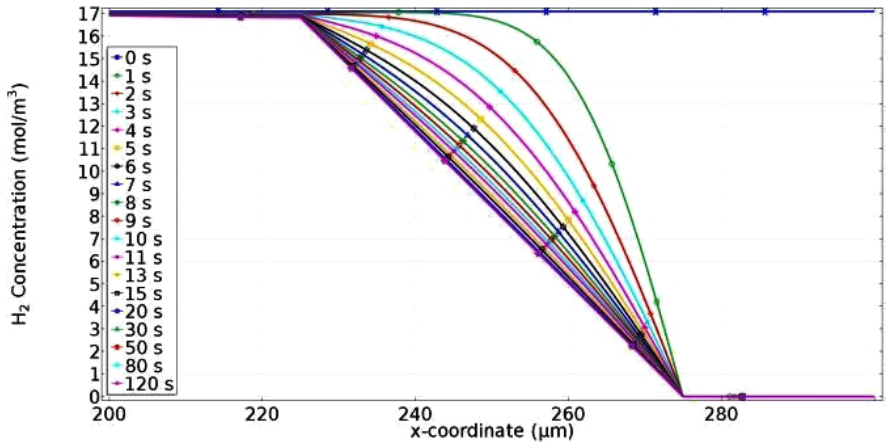

Fig. 4. Concentration profiles of H_2 in the electrolyte phase at different times.

layer compares to the hydrogen concentration change on the anode side.

After reaching steady state condition plotting voltage of the cell vs. current obtained from eq. 8 give a curve called the polarization curve and it is considered characteristic of the fuel cell. Fig. 6 is the polarization curve derived from the model of the MEA with a SPEEK membrane vs. experimental data reported in the literature [39]. To show the accuracy of the developed model, as seen in the Fig.6 , the polarization curve of the cell obtained by the model and from experimental data reported in the literature, was compared. The average absolute relative error percent (AARE%) of this data is 13%. This value

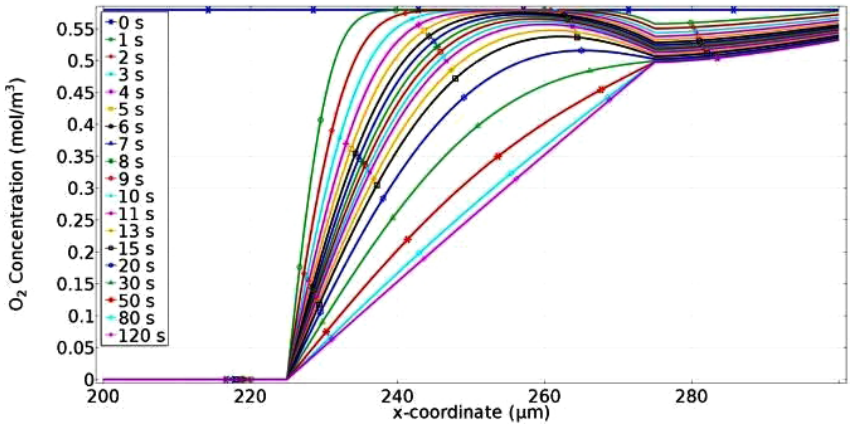

Fig. 5. Concentration profiles of O_2 in the electrolyte phase at different times.

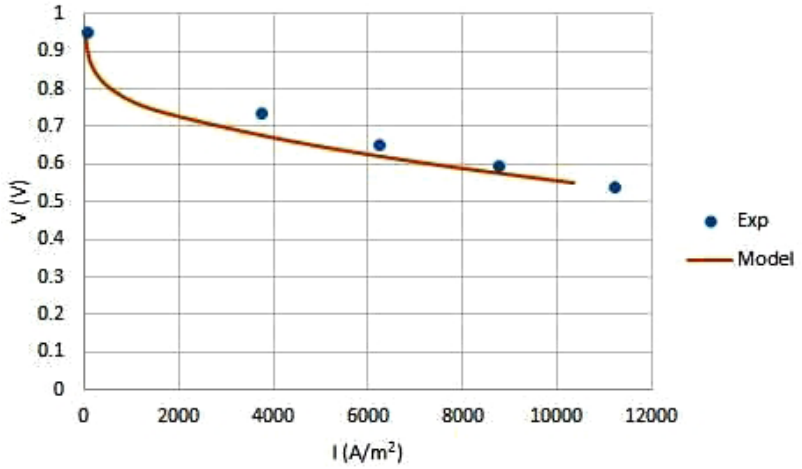

Fig. 6. Polarization curve of the MEA with SPEEK membrane obtained from the model vs. experimental data reported in [39].

MEA with a SPEEK membrane vs. experimental data reported in the literature [39]. To show the accuracy of the developed model, as seen in the Fig. , the polarization curve of the cell obtained by the model and from experimental data reported in the literature, was compared. The average absolute relative error percent (AARE%) of this data is 13%. This value of error showed that the model has a significant agreement with experimental data.

Fig. 7 and Fig. 8 represent the temperature and pressure variation across the MEA. The feed gases are fed to the MEA at atmospheric pressure and 75°C. As it can be observed, both temperature and pressure are only slightly affected or differed through the cell. The temperature increased in the cell from the feed point to the center point. Sensible heat produced from the electrochemical reactions and the heat produced due to total power dissipation have been considered as the heat source. Pressure decreases in each side of the cell from the feed point to the membrane. Depletion of the feed spices that are consumed by the electrochemical reactions are the primary cause of this pressure decline. A pressured variation would be driving force for the cross-sectional velocity which was calculated by the Darcy equation.

Finally, in Fig. 9 a comparison between two polarization curves is presented. One is the MEA working with a SPEEK membrane and the other with a Nafion membrane, both are obtained from the model. The Nafion membrane has higher proton conduction; hence, it is expected to show less ohmic loss, which is compatible with the model result. Another significant difference that is observed in the graph is the higher limiting current density of the Nafion MEA. This dispute arises from the

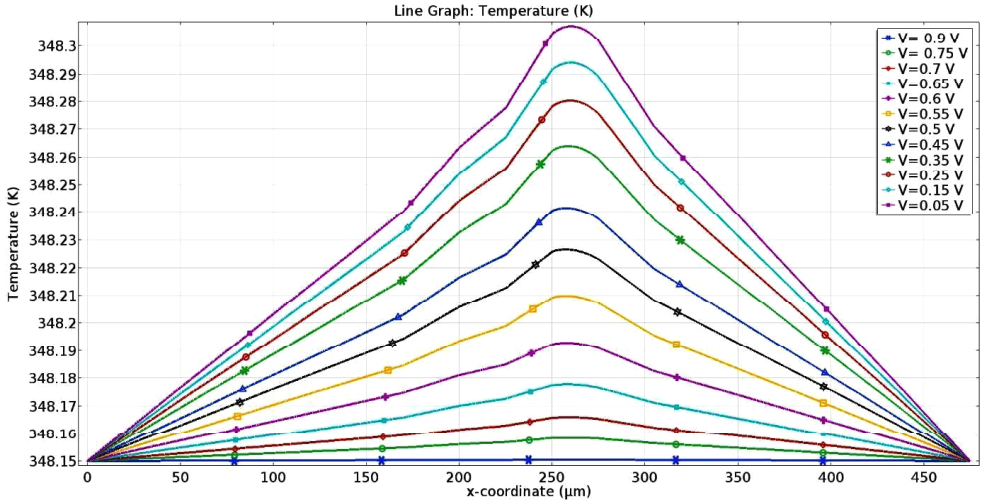

Fig. 7. Temperature profile along the MEA working with a SPEEK membrane.

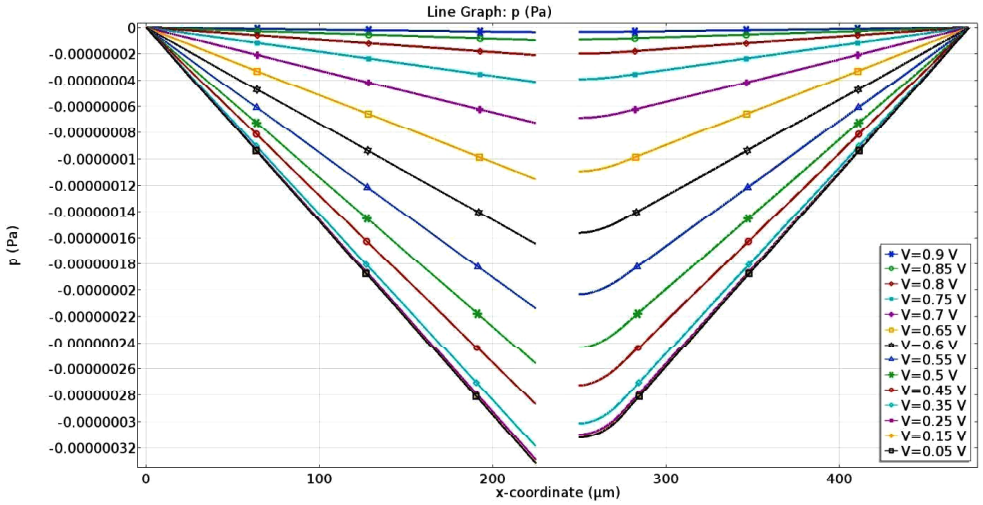

Fig. 8. Pressure profile along the MEA working with a SPEEK membrane in different voltages.

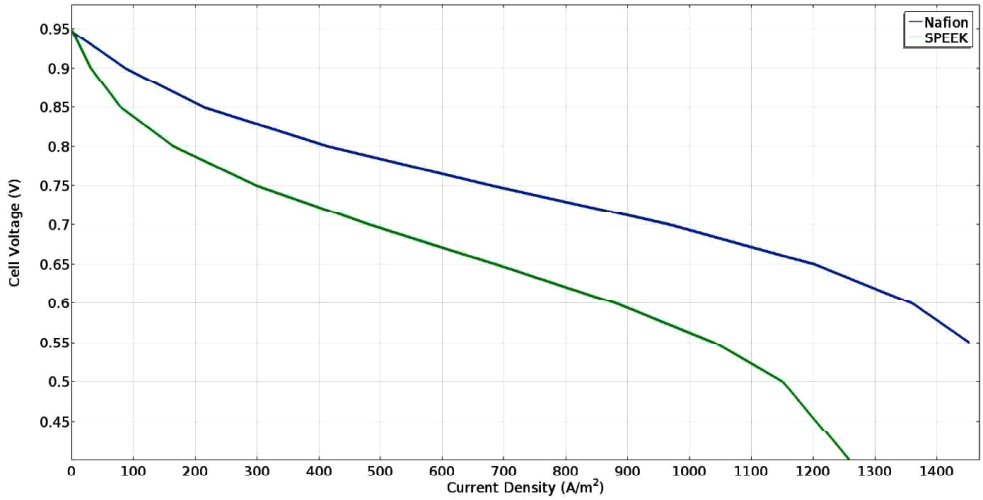

Fig. 9. Comparison of the polarization curve of an MEA working with a SPEEK and Nafion membrane (model results). Feed gases: H_2/ air atmospheric pressure working in 70°C and 80% relative humidity.

higher feed gas permeation of the Nafion membrane in comparison with the SPEEK. Limiting current density is due to limited feed spices reaching the catalyst surface. Higher feed gases solve to the ionomer phase and diffusing through the catalyst surface would cause less electrochemical reaction restriction by the mass transfer of these spices. Hence, higher is the limiting current density would be higher in this case. However, the higher permeation of these feed gases through the membrane also leads to higher feed gas crossover and eventually results in higher chemical degradation of the membrane.

5. Conclusion

With the aim of better understanding nonfluorinated hydrocarbon PEMFC, a model of an MEA with a SPEEK membrane is presented in this work. The model accounts for mass, momentum and charge transfer in different layers of an MEA. The highlight was to consider both gas and electrolyte phase and the inter-phase mass transfer occurring in the catalyst layers. The electrolyte phase presented both in the CL and membrane is considered to be SPEEK, which is a hydrocarbon non-fluorinated PEM and is one of the distinguished low-cost alternatives for Nafion. Furthermore, the model is validated against experimental data. Compatibility of the model results with empirical data shows that this model can be used to predict the performance of MEA with SPEEK in different operating conditions. The dynamic nature of the presented model makes it possible to consider gas cross over during the process of an MEA and is the first step to build a model showing the decay in the performance of the SPEEK MEA in long runs.

References

[1] Ohira A. and Kuroda S., "Differences in the oxygen permeation behavior of perfluorinated and hydrocarbon-type polymer electrolyte membranes at elevated temperatures," Eur. Polym. J., 2015, 67: 78.

[2] Dai H., Guan R., Li C., and Liu J., "Development and characterization of sulfonated poly(ether sulfone) for proton exchange membrane materials," Solid State Ionics, 2007, 178: 339.

[3] Kim Y. S., Einsla B., Sankir M., Harrison W., and Pivovar B. S., "Structure–property–performance relationships of sulfonated poly(arylene ether sulfone)s as a polymer electrolyte for fuel cell applications," Polymer, 2006, 47: 4026.

[4] Matsumoto K., Higashihara T., and Ueda M., "Locally and Densely Sulfonated Poly(ether sulfone)s as Proton Exchange Membrane," Macromolecules, 2009, 42: 1161.

[5] Bae B. et al., "Sulfonated Poly(arylene ether sulfone ketone) Multiblock Copolymers with Highly Sulfonated Blocks. Long-Term Fuel Cell Operation and Post-Test Analyses," ACS Applied Materials & Interfaces, 2011, 3: 2786.

[6] Bae B., Miyatake K., and Watanabe M., "Sulfonated Poly(arylene ether sulfone ketone) Multiblock Copolymers with Highly Sulfonated Block. Synthesis and Properties," Macromolecules, 2010, 43: 2684.

[7] Parcero E., Herrera R., and Nunes S. P., "Phosphonated and sulfonated polyhphenylsulfone membranes for fuel cell application," Journal of Membrane Science, 2006, 285: 206.

[8] Karlsson L. E. and Jannasch P., "Polysulfone ionomers for proton-conducting fuel cell membranes: 2. Sulfophenylated polysulfones and polyphenylsulfones," Electrochimica Acta, 2005, 50: 1939.

[9] Aoki M., Asano N., Miyatake K., Uchida H., and Watanabe M., "Durability of sulfonated polyimide membrane evaluated by long-term polymer electrolyte fuel cell operation," J. Electrochem. Soc., 2006, 153: A1154.

[10] Perrot C., Gonon L., Marestin C., and Gebel G., "Hydrolytic degradation of sulfonated polyimide

membranes for fuel cells," Journal of Membrane Science, 2011, 379: 207.

[11] Pu H. and Liu Q., "Methanol permeability and proton conductivity of polybenzimidazole and sulfonated polybenzimidazole," Polym. Int., 2004, 53: 1512.

[12] Xu H., Chen K., Guo X., Fang J., and Yin J., "Synthesis of novel sulfonated polybenzimidazole and preparation of cross-linked membranes for fuel cell application," Polymer, 2007, 48: 5556.

[13] Huang R. Y. M., Shao P., Burns C. M., and Feng X., "Sulfonation of poly(ether ether ketone)(PEEK): Kinetic study and characterization," J. Appl. Polym. Sci., 2001, 82: 2651.

[14] Gil M., Ji X., Li X., Na H., Eric Hampsey J., and Lu Y., "Direct synthesis of sulfonated aromatic poly(ether ether ketone) proton exchange membranes for fuel cell applications," Journal of membrane science, 2004, 234: 75.

[15] Xing P., Robertson G. P., Guiver M. D., Mikhailenko S. D., Wang K., and Kaliaguine S., "Synthesis and characterization of sulfonated poly(ether ether ketone) for proton exchange membranes," Journal of membrane science, 2004, 229: 95.

[16] Muthu Lakshmi R. T. S., Choudhary V., and Varma I. K., "Sulphonated poly(ether ether ketone): Synthesis and characterisation," Journal of Materials Science, 2005, 40: 629.

[17] Parnian M. J., Rowshanzamir S., and Gashoul F., "Comprehensive investigation of physicochemical and electrochemical properties of sulfonated poly (ether ether ketone) membranes with different degrees of sulfonation for proton exchange membrane fuel cell applications," Energy, 2017, 125: 614.

[18] He S., Lin Y., Ma H., Jia H., Liu X., and Lin J., "Preparation of sulfonated poly(ether ether ketone) (SPEEK) membrane using ethanol/water mixed solvent," Mater. Lett., 2016, 169: 69.

[19] Carbone A., Pedicini R., Portale G., Longo A., D'Ilario L., and Passalacqua E., "Sulphonated poly(ether ether ketone) membranes for fuel cell application: Thermal and structural characterisation," J. Power Sources, 2006, 163: 18.

[20] Do K. N. T. and Kim D., "Synthesis and characterization of homogeneously sulfonated poly(ether ether ketone) membranes: Effect of casting solvent," J. Appl. Polym. Sci., 2008, 110: 1763.

[21] Li W., Zhang F., Yi S., Huang C., Zhang H., and Pan M., "Effects of casting solvent on microstructrue and ionic conductivity of anhydrous sulfonated poly(ether ether ketone)-inoic liquid composite membranes," Int. J. Hydrogen Energy, 2012, 37: 748.

[22] Jun M.-S., Choi Y.-W., and Kim J.-D., "Solvent casting effects of sulfonated poly(ether ether ketone) for Polymer electrolyte membrane fuel cell," Journal of Membrane Science, 2012, 396: 32.

[23] Li X. et al., "Fabrication of sulfonated poly(ether ether ketone ketone) membranes with high proton conductivity," Journal of Membrane Science, 2006, 281: 1.

[24] Lee J. K., Li W., and Manthiram A., "Sulfonated poly(ether ether ketone) as an ionomer for direct methanol fuel cell electrodes," J. Power Sources, 2008, 180: 56.

[25] Yang B. and Manthiram A., "Sulfonated Poly(ether ether ketone) Membranes for Direct Methanol Fuel Cells," Electrochem. Solid-State Lett., 2003, 6: A229.

[26] Sayadi P., Rowshanzamir S., and Parnian M. J., "Study of hydrogen crossover and proton conductivity of self-humidifying nanocomposite proton exchange membrane based on sulfonated poly (ether ether ketone)," Energy, 2016, 94: 292.

[27] Anderson K. et al., "Infrared spectroscopy of ion-induced cross-linked sulfonated poly(ether ether ketone)," Polymer, 2016, 93: 65.

[28] Zhao Y.-y., Tsuchida E., Choe Y.-K., Ikeshoji T.,

Barique M. A., and Ohira A., "Ab initio studies on the proton dissociation and infrared spectra of sulfonated poly(ether ether ketone) (SPEEK) membranes," Phys. Chem. Chem. Phys., 2014, 16: 1041.

[29] Mahajan C. V. and Ganesan V., "Atomistic Simulations of Structure of Solvated Sulfonated Poly(ether ether ketone) Membranes and Their Comparisons to Nafion: I. Nanophase Segregation and Hydrophilic Domains," The Journal of Physical Chemistry B, 2010, 114: 8357.

[30] Komarov P. V., Veselov I. N., Chu P. P., Khalatur P. G., and Khokhlov A. R., "Atomistic and mesoscale simulation of polymer electrolyte membranes based on sulfonated poly(ether ether ketone)," Chem. Phys. Lett., 2010, 487: 291.

[31] Weber A. Z. et al., "A Critical Review of Modeling Transport Phenomena in Polymer-Electrolyte Fuel Cells," J. Electrochem. Soc., 2014, 161: F1254.

[32] Poornesh K. K. and Cho C., "Stability of Polymer Electrolyte Membranes In Fuel Cells: Initial Attempts To Bridge Physical And Chemical Degradation Modes," Fuel Cells, 2015, 15: 196.

[33] Qin C. Z. and Hassanizadeh S. M., "A new approach to modelling water flooding in a polymer electrolyte fuel cell," Int. J. Hydrogen Energy, 2015, 40: 3348.

[34] Cao T.-F., Mu Y.-T., Ding J., Lin H., He Y.-L., and Tao W.-Q., "Modeling the temperature distribution and performance of a PEM fuel cell with thermal contact resistance," Int. J. Heat Mass Transfer, 2015, 87: 544.

[35] Chippar P. and Ju H., "Numerical modeling and investigation of gas crossover effects in high temperature proton exchange membrane (PEM) fuel cells," Int. J. Hydrogen Energy, 2012.

[36] Chippar P. and Ju H., "Three-dimensional non-isothermal modeling of a phosphoric acid-doped polybenzimidazole (PBI) membrane fuel cell," Solid State Ionics, 2012, 225: 30.

[37] Knauth P. and Di Vona M. L., "Hydration and proton conductivity of ionomers: the model case of Sulfonated Aromatic Polymers," Frontiers in Energy Research, 2014, 2.

[38] Cheddie D. and Munroe N., "Review and comparison of approaches to proton exchange membrane fuel cell modeling," J. Power Sources, 2005, 147: 72.

[39] Qiu X., Dong T., Ueda M., Zhang X., and Wang L., "Sulfonated reduced graphene oxide as a conductive layer in sulfonated poly(ether ether ketone) nanocomposite membranes," Journal of Membrane Science, 2017, 524: 663.